



Virginia Museum of  
**NATURAL HISTORY**

———— PUBLICATIONS ————

# *JEFFERSONIANA*

*Contributions from the  
Virginia Museum of Natural History*

---

Number 25

19 November 2010

## Reconnaissance Mineralogy of the Eocene Mole Hill Diatreme, Rockingham County, Virginia

James S. Beard

ISSN 1061-1878

Virginia Museum of Natural History  
Scientific Publications Series

The Virginia Museum of Natural History produces five scientific publication series, with each issue published as suitable material becomes available and each numbered consecutively within its series. Topics consist of original research conducted by museum staff or affiliated investigators based on the museum's collections or on subjects relevant to the museum's areas of interest. All are distributed to other museums and libraries through our exchange program and are available for purchase by individual consumers.

Memoirs are typically larger productions: individual monographs on a single subject such as a regional survey or comprehensive treatment of an entire group. The standardized format is an 8.5 x 11 inch page with two columns.

*Jeffersoniana* is an outlet for relatively short studies treating a single subject, allowing for expeditious publication. The standardized format is a single column on a 6 x 9 inch page.

Guidebooks are publications, often semi-popular, designed to assist readers on a particular subject in a particular region. They may be produced to accompany members of an excursion or may serve as a field guide for a specific geographic area.

Special Publications consist of unique contributions, usually book length, either single-subject or the proceedings of a symposium or multi-disciplinary project in which the papers reflect a common theme. Appearance and format are customized to accommodate specific needs; page size and layout varies accordingly.

*The Insects of Virginia* is a series of bulletins emphasizing identification, distribution, and biology of individual taxa (usually a family) of insects as represented in the Virginia fauna. Originally produced at VPI & SU in a 6 x 9 inch page size, the series was adopted by VMNH in 1993 and issued in a redesigned 8.5 x 11 inch, double column format.

Copyright 2010 by the Virginia Museum of Natural History  
Printed in the United States of America  
ISSN 1061-1878

## Reconnaissance Mineralogy of the Eocene Mole Hill Diatreme, Rockingham County, Virginia

JAMES S. BEARD

Virginia Museum of Natural History  
21 Starling Avenue  
Martinsville, Virginia 24112, USA  
jim.beard@vmnh.virginia.gov

### ABSTRACT

The Mole Hill diatreme consists of picobasalt with abundant megacrysts (0.5 mm to 2cm in maximum dimension) of clinopyroxene, Mg-Al-Fe spinel, and (less abundant) olivine. Cognate minerals include microphenocryst and groundmass plagioclase, olivine, clinopyroxene and Fe-Ti-(Cr) spinel. Clinopyroxene is the most abundant megacryst phase. Overall, the clinopyroxene in the megacryst cores is a high-Al, low-Cr augite with Mg# 78-88. Sieve textured rims approach groundmass clinopyroxene compositions. Olivine occurs as megacrysts and also as small (0.1- 0.5 mm) crystals of indeterminate origin. These may be phenocrysts, xenocrysts, or both. All non-groundmass olivine is zoned, becoming Fe- and Ca-rich (and approaching the composition of groundmass olivine) rimward. The most primitive olivine has Fo~90 and NiO as high as 0.75wt.%. More typically, olivine is Fo78-88 with NiO <0.5 wt.%. The megacryst/xenocryst olivine cores have higher Mg# and lower CaO than groundmass olivine. Megacrystic spinels are notably low in Cr, with Cr# <1, and variable Mg# ranging from 52-74. This variation appears to be continuous, despite the lack of zoning in individual spinel xenocrysts. Plagioclase occurs only as a microphenocryst phase, with uniform An75 cores and rims as sodic as An58. Cognate clinopyroxene (Mg#67-78) is enriched in Ca and Ti relative to the megacrysts. Groundmass olivine has low NiO and high (0.3-0.6 wt.%) CaO. Groundmass spinels have ulvospinel contents near 50%, initially rising with Mg# (in Cr-rich microphenocrysts) then dropping. Although the lack of context for the megacrysts precludes a definitive understanding of their origin, megacryst chemistry (especially the low-Cr spinels and the overall abundance of clinopyroxene) suggests a clinopyroxene-rich source in the upper (e.g. spinel zone) continental lithosphere. This source is likely similar to the Al-augite suite clinopyroxenites and wehrlites that occur as xenoliths and as intrusive veins in composite xenoliths from alkali basalt provinces worldwide. Cognate mineral (groundmass minerals and microphenocrysts) compositions are consistent with crystallization from a slightly evolved alkali basalt melt.

### INTRODUCTION

A localized series of Eocene alkaline subvolcanic necks, pipes, and dikes (Eocene Subvolcanic Suite, ESS) outcrops in Highland County, Virginia and adjacent Pendleton County, West Virginia (Rader et al., 1986; Southworth et al., 1993). A single isolated volcanic plug, Mole Hill, outcrops in Rockingham County, Virginia 60 km east of the main field (Fig. 1).

The suite is intrusive into folded sedimentary rocks of Paleozoic age. The rocks of the ESS range in composition from picobasalt to rhyolite. Basaltic rocks are nepheline-normative and plot in the field of alkaline within-plate basalt (Wood 1980; Southworth et al., 1993). Available bulk element and isotope chemistry is consistent with a mantle

origin for the suite with little evidence for crustal contamination aside from obvious xenoliths of high-level lithologies (e.g. Paleozoic limestone and sandstone) (Southworth et al., 1993; Tso et al., 2004; Tso and Surber, 2006). The more silicic rocks of the ESS appear to have been emplaced during explosive eruptions, as borne out by the presence of breccia pipes and peperites (Rader et al., 1986; Tso and Surber, 2006) and by the recognition of correlative volcanic ash deposits in the Eocene rocks of the North Carolina Coastal Plain (Harris and Fullagar, 1989). Several of the mafic plugs, including Mole Hill, have been interpreted as diatremes. Although the tectonic setting for the emplacement of these rocks is far from obvious, they seem to follow a NW-trending lineament associated with a NW trending fracture set. This may indicate emplacement along reactivated orogen-parallel faults. Southworth et al. (1993) suggest that this reactivation is related to extension accompanying plate reorganizations between 37 and 53Ma.

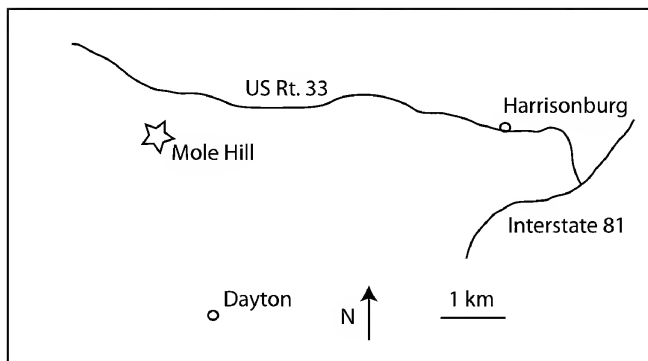


**Figure 1:** Location of Mole Hill in Rockingham County, Virginia.

The Mole Hill diatreme consists of alkali olivine microbasalt (tentative designation based on limited data) containing abundant large (0.5 mm to 2cm; large in the context of the host basalt) crystals of olivine, spinel and clinopyroxene (henceforth referred to as megacrysts) in a largely crystalline groundmass consisting of olivine, clinopyroxene, plagioclase, and Fe-Ti oxides. This study encompasses the description of the composition and compositional variability in the crystalline phases of the Mole Hill microbasalt including some interpretation of the origin of the megacryst phases.

## Petrography and Mineral Chemistry

**Methods.** Minerals were analyzed using the Cameca SX-50 electron microprobe in the Department of Geological Sciences at Virginia Polytechnic Institute and State University. Beam current was 15na, at 20kv; spot size was 3-5 microns. Counting times were 20 seconds on peak and 10 seconds on two background points. A variety of natural and synthetic silicates and oxides were used as standards.

**General.** The basalt at Mole Hill is a alkali olivine microbasalt characterized by megacrysts of olivine, clinopyroxene, and aluminous spinel with a microphenocrysts of plagioclase, olivine, clinopyroxene and Fe-Ti-(Cr) oxides in a fine-grained holocrystalline groundmass of the same mineralogy. A weak to moderate alignment of plagioclase laths is apparent in some samples.

**Olivine.** Olivine occurs as megacrysts, a groundmass phase, and in crystals of intermediate size (0.1-0.5 mm) of, apparently, mixed xenocrystic/phenocrystic origin.

Megacryst/xenocryst cores range in (average) composition from Fo<sub>82</sub>-Fo<sub>90</sub> (Table 1, Fig. 2). NiO content ranges from 0.2-0.6 wt.%, with some spot analyses in the most magnesian megacryst >0.7wt.% (Fig. 2). CaO concentrations in the megacrysts/xenocryst cores are <0.3 wt.% (Fig. 2) The megacrysts are zoned, with rims approaching groundmass olivine compositions and intermediate areas that may have partially equilibrated with the

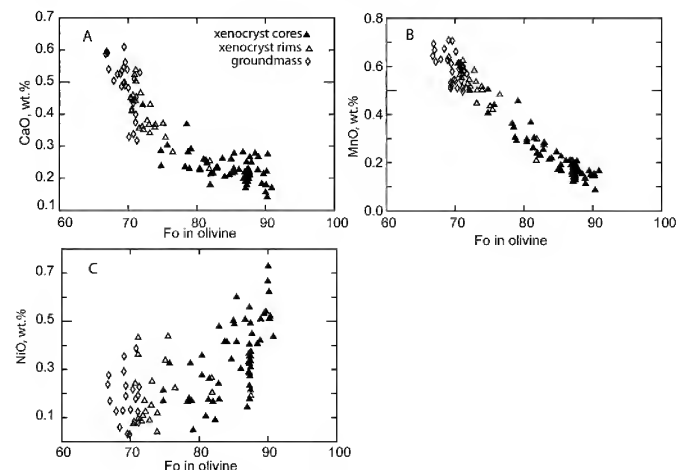


**Figure 2.** Variations in olivine chemistry, Mole Hill megacrysts and groundmass.

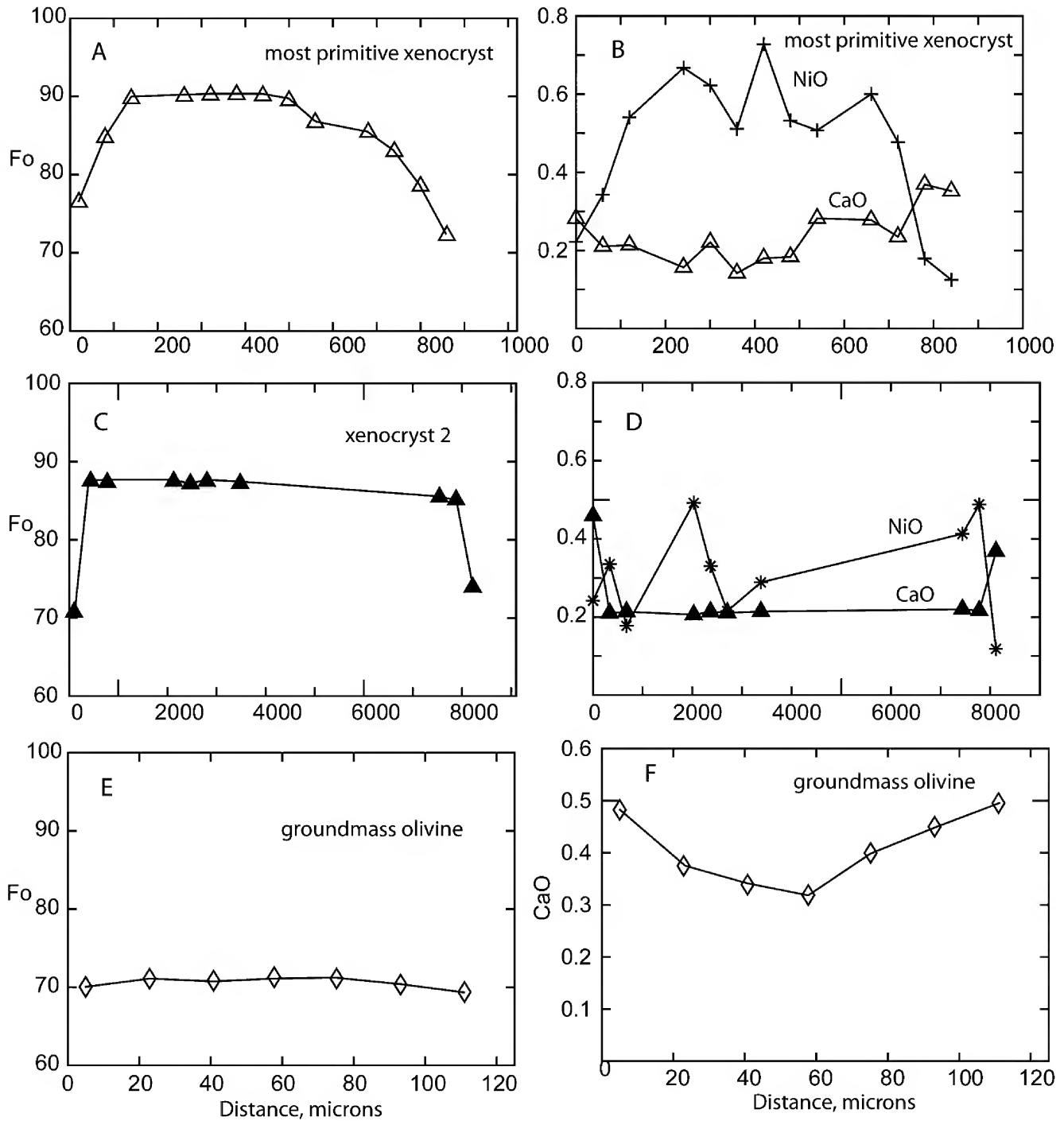


**Figure 3.** Chemical variation with distance along microprobe traverses in olivine. A, B. Most magnesian xenocryst. C, D. Large (1 cm) xenocryst. E, F. Microphenocryst.

Table 1. Olivine

| VMNH #                   | 81554    | 81564    | 81564  | 81554    | 81554    | 81564  | 81564  | 81564  | 81554    | 81554    |
|--------------------------|----------|----------|--------|----------|----------|--------|--------|--------|----------|----------|
| sample                   | Mh 1-5-1 | Mh 11    | Mh 11  | Mh 1-5-2 | Mh 1-5-2 | Mh 11  | Mh 11  | Mh 11  | Mh 1-5-1 | Mh 1-5-2 |
| N                        | 6        | 16       | 1      | 5        | 6        | 3      | 12     | 4      | 4        | 5        |
| X'l type                 | mega     | mega     | Mega   | mega     | zoned    | mega   | phen   | gmass  | gmass    | gmass    |
| notes                    | core     | v. large |        | core     | core     | rim    |        |        |          |          |
| SiO <sub>2</sub>         | 40.49    | 41.31    | 41.04  | 42.06    | 40.35    | 38.45  | 38.32  | 37.89  | 36.98    | 37.58    |
| MgO                      | 45.60    | 47.63    | 47.21  | 49.52    | 43.41    | 37.50  | 35.76  | 33.64  | 34.08    | 34.23    |
| CaO                      | 0.25     | 0.21     | 0.25   | 0.18     | 0.25     | 0.40   | 0.44   | 0.58   | 0.48     | 0.51     |
| FeO                      | 13.01    | 12.29    | 11.56  | 9.87     | 16.97    | 24.41  | 26.81  | 28.70  | 26.72    | 28.04    |
| MnO                      | 0.20     | 0.16     | 0.17   | 0.15     | 0.27     | 0.50   | 0.56   | 0.64   | 0.65     | 0.65     |
| NiO                      | 0.39     | 0.31     | na     | 0.60     | 0.25     | 0.23   | 0.18   | 0.18   | 0.11     | 0.01     |
| sum                      | 99.93    | 101.92   | 100.23 | 102.38   | 101.50   | 101.49 | 102.07 | 101.62 | 99.01    | 101.02   |
| <b>Cations/4 oxygens</b> |          |          |        |          |          |        |        |        |          |          |
| Si                       | 1.007    | 1.003    | 1.008  | 1.006    | 1.006    | 0.996  | 0.998  | 1.001  | 0.997    | 0.996    |
| Mg                       | 1.691    | 1.725    | 1.728  | 1.766    | 1.614    | 1.448  | 1.389  | 1.325  | 1.370    | 1.352    |
| Ca                       | 0.007    | 0.006    | 0.007  | 0.005    | 0.007    | 0.011  | 0.012  | 0.016  | 0.014    | 0.015    |
| Fe                       | 0.271    | 0.250    | 0.237  | 0.197    | 0.354    | 0.529  | 0.584  | 0.634  | 0.602    | 0.622    |
| Mn                       | 0.004    | 0.003    | 0.004  | 0.003    | 0.006    | 0.011  | 0.012  | 0.014  | 0.015    | 0.015    |
| Ni                       | 0.008    | 0.006    | na     | 0.012    | 0.005    | 0.005  | 0.004  | 0.004  | 0.002    | 0.000    |
| total                    | 2.988    | 2.992    | 2.984  | 2.990    | 2.992    | 3.001  | 2.999  | 2.996  | 3.000    | 3.000    |
| Fo                       | 86.2     | 87.4     | 87.9   | 89.9     | 82.0     | 73.2   | 70.4   | 67.6   | 69.5     | 68.5     |

host basalt (e.g. Costa and Dungan, 2005) (Fig. 3). The low CaO and high NiO concentrations in the megacryst cores suggest that the megacrystic olivines are mantle xenocrysts that did not form in equilibrium with the host basalt (Simkin and Smith, 1970; Hirano et al., 2004; Rohrbach et al., 2005). Groundmass and (micro)phenocrystic olivine is substantially more Fe-rich (Fo<sub>68-80</sub>) CaO-rich (CaO = 0.3-0.6 wt.%) and NiO-poor (NiO concentrations are usually below 0.3 wt. % with many values approaching detection limits (0.1 wt.%) than the megacryst cores (Table 1; Fig. 2). Zoning in true microphenocrysts is limited (i.e. Fo<sub>71-68</sub>; Fig. 3). More strongly zoned intermediate size and composition crystals (e.g. Fo<sub>80-70</sub>) may either reflect an early phenocryst phase or partially re-equilibrated xenocrysts.

**Clinopyroxene.** Clinopyroxene is the most abundant megacryst and groundmass phase in the Mole Hill microbasalt. There are four chemically distinct populations of clinopyroxene in the Mole Hill microbasalt, with two of these represented by a single analyzed crystal. Most clinopyroxene megacrysts are high-Al (5.6-8.8 wt.% Al<sub>2</sub>O<sub>3</sub>) augites with TiO<sub>2</sub> <1.0 wt.% and Na<sub>2</sub>O between 0.4-0.9 wt.% (Table 2; Fig. 4). Mg#'s of megacryst cores (average) range from 78-86. The most magnesian and Cr-rich clinopyroxene occurs in a two-crystal

“xenolith” with a large olivine xenocryst (Figure 4). The other analyzed xenocrysts vary in Mg# (Figs. 4,5), and can be characterized as low-Cr (e.g. Cr<sub>2</sub>O<sub>3</sub> <0.2 wt.%). Most xenocrysts are zoned, with the sieve-textured rims approaching groundmass clinopyroxene composition. Groundmass clinopyroxene has Mg# near 70. It can be described as salite (Ca-rich augite) and is higher in Ti and, for the most part, lower in Al than the megacrysts. Some groundmass clinopyroxenes (and megacryst rims) have fairly high (>0.3 wt.%) Cr<sub>2</sub>O<sub>3</sub> (Table 2; Fig. 4).

Two unusual clinopyroxene xenocrysts were analyzed. One has the low Mg# typical of groundmass clinopyroxene, but is distinctly lower in Ti and enriched in Na and Si with respect to the groundmass clinopyroxene (Table 2, Fig. 4). The other unique xenocryst is exceptionally enriched in Ti, Al and Ca, containing among the highest concentrations of these elements ever reported (Robinson, 1980) (Table 2). Similar high-Al pyroxenes have been reported as phenocrysts in alkaline igneous rocks (e.g. Gerke et al., 2005). This grain has a sieve-textured rim, suggesting reaction with the microbasalt host, and a xenocrystic (or, possibly, high-P phenocrystic) origin seems likely.

**Spinel.** Aluminous spinels (85-95% aluminous (i.e. sp + hc) end-member) occur as large (up to 5

Table 2: Clinopyroxene

| VMNH #                   | 81554    | 81554    | 81554    | 81554     | 81554    | 81554    | 81554    | 81554    | 81554    | 81554    | 81554    | 81554     | 81554      | 81554      | 81554      | 81554      | 81554      | 81564      | 81564      | 81564      | 81564      | 81564      | 81564      | 81564      | 81564      |            |        |
|--------------------------|----------|----------|----------|-----------|----------|----------|----------|----------|----------|----------|----------|-----------|------------|------------|------------|------------|------------|------------|------------|------------|------------|------------|------------|------------|------------|------------|--------|
| sample                   | Mh 1-5-1 | Mh 1-5-2 | Mh 1-5-2 | Mh 1-5-1  | Mh 1-5-1 | Mh 1-5-1 | Mh 1-5-1 | Mh 1-5-1 | Mh 1-5-1 | Mh 1-5-1 | Mh 1-5-1 | Mh 1-5-1  | Mh 1-5-1   | Mh 1-5-1   | Mh 1-5-1   | Mh 1-5-1   | Mh 1-5-1   | Mh 1-5-1   | Mh 1-5-1   | Mh 1-5-1   | Mh 1-5-1   | Mh 1-5-1   | Mh 1-5-1   | Mh 1-5-1   | Mh 1-5-1   |            |        |
| n                        | 9        | 7        | 7        | 11        | 1        | 1        | 10       | 10       | 12       | 4        | 4        | 12        | 10         | 5          | 5          | 11         | 4          | 4          | 4          | 5          | 5          | 3          | 5          | 5          | 5          |            |        |
| x'l type                 | mega     | mega     | mega     | mega      | mega     | mega     | mega     | mega     | Xeno     | Xeno     | Xeno     | *xeno cpx | mega       | mega       | mega       | mega       | mega       | mega       | mega       | mega       | mega       | mega       | mega       | mega       | mega       |            |        |
| notes                    |          |          | core     | intermed. | Rim      |          |          |          | low-Al   | low-Al   | low-Al   | high-Al   | in ol xeno | in ol xeno | in ol xeno | mega (rim) | mega (rim) | mega (rim) | mega (rim) | mega (rim) | mega (rim) | mega (rim) | mega (rim) | mega (rim) | mega (rim) | mega (rim) |        |
| SiO2                     | 49.90    | 50.22    | 48.93    | 48.75     | 48.25    | 50.58    | 40.19    | 50.28    | 40.19    | 50.58    | 40.19    | 40.19     | 50.28      | 49.04      | 48.76      | 48.63      | 48.63      | 48.63      | 48.63      | 48.63      | 48.63      | 48.63      | 48.63      | 48.63      | 48.63      | 48.63      | 48.26  |
| Al2O3                    | 7.72     | 6.17     | 8.38     | 8.47      | 5.01     | 3.24     | 14.00    | 5.96     | 14.00    | 3.24     | 14.00    | 14.00     | 5.96       | 5.57       | 8.78       | 4.05       | 4.05       | 4.05       | 4.05       | 4.05       | 4.05       | 4.05       | 4.05       | 4.05       | 4.05       | 4.05       | 5.30   |
| Na2O                     | 0.65     | 0.53     | 0.90     | 0.82      | 0.50     | 1.03     | 0.24     | 0.53     | 0.24     | 1.03     | 0.24     | 0.24      | 0.53       | 0.43       | 0.78       | 0.47       | 0.47       | 0.47       | 0.47       | 0.47       | 0.47       | 0.47       | 0.47       | 0.47       | 0.47       | 0.47       | 0.47   |
| MgO                      | 16.53    | 15.43    | 15.17    | 14.68     | 13.20    | 12.58    | 9.82     | 16.54    | 9.82     | 12.58    | 9.82     | 9.82      | 16.54      | 14.61      | 15.02      | 12.65      | 12.65      | 12.65      | 12.65      | 12.65      | 12.65      | 12.65      | 12.65      | 12.65      | 12.65      | 12.65      | 12.66  |
| CaO                      | 18.68    | 21.65    | 18.42    | 19.45     | 23.44    | 21.54    | 24.74    | 20.94    | 24.74    | 21.54    | 24.74    | 24.74     | 20.94      | 22.52      | 19.69      | 22.43      | 22.43      | 22.43      | 22.43      | 22.43      | 22.43      | 22.43      | 22.43      | 22.43      | 22.43      | 22.43      | 22.92  |
| TiO2                     | 0.48     | 0.84     | 0.71     | 0.81      | 1.47     | 0.38     | 4.20     | 0.46     | 4.20     | 0.38     | 4.20     | 4.20      | 0.46       | 1.02       | 0.76       | 1.71       | 1.71       | 1.71       | 1.71       | 1.71       | 1.71       | 1.71       | 1.71       | 1.71       | 1.71       | 1.71       | 1.95   |
| FeO                      | 5.48     | 5.96     | 7.42     | 7.26      | 7.67     | 10.51    | 7.02     | 4.69     | 7.02     | 10.51    | 7.02     | 7.02      | 4.69       | 6.21       | 6.55       | 9.32       | 9.32       | 9.32       | 9.32       | 9.32       | 9.32       | 9.32       | 9.32       | 9.32       | 9.32       | 9.32       | 8.73   |
| MnO                      | 0.11     | 0.15     | 0.16     | 0.16      | 0.10     | 0.15     | 0.11     | 0.11     | 0.11     | 0.15     | 0.11     | 0.11      | 0.11       | 0.14       | 0.15       | 0.24       | 0.24       | 0.24       | 0.24       | 0.24       | 0.24       | 0.24       | 0.24       | 0.24       | 0.24       | 0.21       | 0.21   |
| Cr2O3                    | 0.18     | 0.04     | 0.03     | 0.02      | 0.00     | 0.07     | 0.00     | 0.61     | 0.00     | 0.07     | 0.00     | 0.00      | 0.61       | 0.47       | 0.04       | 0.01       | 0.01       | 0.01       | 0.01       | 0.01       | 0.01       | 0.01       | 0.01       | 0.01       | 0.01       | 0.01       | 0.14   |
| sum                      | 99.74    | 100.97   | 100.12   | 100.41    | 99.66    | 100.09   | 100.30   | 100.12   | 100.30   | 100.09   | 100.30   | 100.30    | 100.12     | 100.04     | 100.54     | 99.52      | 99.52      | 99.52      | 99.52      | 99.52      | 99.52      | 99.52      | 99.52      | 99.52      | 99.52      | 99.52      | 100.64 |
| <b>Cations/6 oxygens</b> |          |          |          |           |          |          |          |          |          |          |          |           |            |            |            |            |            |            |            |            |            |            |            |            |            |            |        |
| Si                       | 1.822    | 1.832    | 1.797    | 1.790     | 1.817    | 1.905    | 1.519    | 1.838    | 1.519    | 1.905    | 1.519    | 1.519     | 1.838      | 1.820      | 1.783      | 1.842      | 1.842      | 1.842      | 1.842      | 1.842      | 1.842      | 1.842      | 1.842      | 1.842      | 1.842      | 1.842      | 1.805  |
| Al                       | 0.332    | 0.265    | 0.363    | 0.366     | 0.222    | 0.144    | 0.624    | 0.257    | 0.624    | 0.144    | 0.624    | 0.624     | 0.257      | 0.244      | 0.378      | 0.181      | 0.181      | 0.181      | 0.181      | 0.181      | 0.181      | 0.181      | 0.181      | 0.181      | 0.181      | 0.181      | 0.234  |
| Na                       | 0.046    | 0.037    | 0.064    | 0.059     | 0.037    | 0.075    | 0.017    | 0.038    | 0.017    | 0.075    | 0.017    | 0.017     | 0.038      | 0.031      | 0.055      | 0.035      | 0.035      | 0.035      | 0.035      | 0.035      | 0.035      | 0.035      | 0.035      | 0.035      | 0.035      | 0.035      | 0.034  |
| Mg                       | 0.900    | 0.839    | 0.831    | 0.804     | 0.741    | 0.707    | 0.553    | 0.902    | 0.553    | 0.707    | 0.553    | 0.553     | 0.902      | 0.808      | 0.819      | 0.714      | 0.714      | 0.714      | 0.714      | 0.714      | 0.714      | 0.714      | 0.714      | 0.714      | 0.714      | 0.714      | 0.706  |
| Ca                       | 0.731    | 0.846    | 0.725    | 0.765     | 0.946    | 0.869    | 1.002    | 0.820    | 1.002    | 0.869    | 1.002    | 1.002     | 0.820      | 0.896      | 0.772      | 0.911      | 0.911      | 0.911      | 0.911      | 0.911      | 0.911      | 0.911      | 0.911      | 0.911      | 0.911      | 0.911      | 0.919  |
| Ti                       | 0.013    | 0.023    | 0.020    | 0.022     | 0.042    | 0.011    | 0.119    | 0.013    | 0.119    | 0.011    | 0.119    | 0.119     | 0.013      | 0.029      | 0.021      | 0.049      | 0.049      | 0.049      | 0.049      | 0.049      | 0.049      | 0.049      | 0.049      | 0.049      | 0.049      | 0.055      |        |
| Fe                       | 0.167    | 0.182    | 0.228    | 0.223     | 0.241    | 0.331    | 0.222    | 0.143    | 0.222    | 0.331    | 0.222    | 0.222     | 0.143      | 0.193      | 0.200      | 0.296      | 0.296      | 0.296      | 0.296      | 0.296      | 0.296      | 0.296      | 0.296      | 0.296      | 0.296      | 0.273      |        |
| Mn                       | 0.004    | 0.005    | 0.005    | 0.005     | 0.003    | 0.005    | 0.003    | 0.004    | 0.003    | 0.005    | 0.003    | 0.003     | 0.004      | 0.004      | 0.005      | 0.008      | 0.008      | 0.008      | 0.008      | 0.008      | 0.008      | 0.008      | 0.008      | 0.008      | 0.008      | 0.007      |        |
| Cr                       | 0.005    | 0.001    | 0.001    | 0.001     | 0.000    | 0.002    | 0.000    | 0.017    | 0.000    | 0.002    | 0.000    | 0.000     | 0.017      | 0.014      | 0.001      | 0.000      | 0.000      | 0.000      | 0.000      | 0.000      | 0.000      | 0.000      | 0.000      | 0.000      | 0.000      | 0.000      | 0.004  |
| total                    | 4.020    | 4.030    | 4.033    | 4.034     | 4.049    | 4.049    | 4.059    | 4.031    | 4.059    | 4.049    | 4.059    | 4.059     | 4.031      | 4.038      | 4.034      | 4.036      | 4.036      | 4.036      | 4.036      | 4.036      | 4.036      | 4.036      | 4.036      | 4.036      | 4.036      | 4.036      | 4.038  |
| AlIV                     | 0.178    | 0.168    | 0.203    | 0.210     | 0.183    | 0.095    | 0.481    | 0.162    | 0.481    | 0.095    | 0.481    | 0.481     | 0.162      | 0.180      | 0.217      | 0.158      | 0.158      | 0.158      | 0.158      | 0.158      | 0.158      | 0.158      | 0.158      | 0.158      | 0.158      | 0.158      | 0.195  |
| AlVI                     | 0.154    | 0.097    | 0.160    | 0.156     | 0.039    | 0.049    | 0.143    | 0.095    | 0.143    | 0.049    | 0.143    | 0.143     | 0.095      | 0.063      | 0.161      | 0.023      | 0.023      | 0.023      | 0.023      | 0.023      | 0.023      | 0.023      | 0.023      | 0.023      | 0.023      | 0.023      | 0.039  |
| Wo                       | 40.6     | 45.3     | 40.6     | 42.7      | 49.0     | 45.6     | 56.4     | 44.0     | 56.4     | 45.6     | 56.4     | 56.4      | 44.0       | 47.2       | 43.1       | 47.4       | 47.4       | 47.4       | 47.4       | 47.4       | 47.4       | 47.4       | 47.4       | 47.4       | 47.4       | 47.4       | 48.4   |
| En                       | 50.0     | 45.0     | 46.6     | 44.9      | 38.4     | 37.1     | 31.2     | 48.3     | 31.2     | 37.1     | 31.2     | 31.2      | 48.3       | 42.6       | 45.8       | 37.2       | 37.2       | 37.2       | 37.2       | 37.2       | 37.2       | 37.2       | 37.2       | 37.2       | 37.2       | 37.2       | 37.2   |
| Fs                       | 9.3      | 9.7      | 12.8     | 12.4      | 12.5     | 17.4     | 12.5     | 7.7      | 12.5     | 17.4     | 12.5     | 12.5      | 7.7        | 10.2       | 11.2       | 15.4       | 15.4       | 15.4       | 15.4       | 15.4       | 15.4       | 15.4       | 15.4       | 15.4       | 15.4       | 15.4       | 14.4   |
| Mg#                      | 84.3     | 82.2     | 78.5     | 78.3      | 75.4     | 68.1     | 71.5     | 86.3     | 71.5     | 68.1     | 71.5     | 71.5      | 86.3       | 80.6       | 80.3       | 70.7       | 70.7       | 70.7       | 70.7       | 70.7       | 70.7       | 70.7       | 70.7       | 70.7       | 70.7       | 70.7       | 72.1   |

\*High calculated Wo reflects high Al rather than high Ca

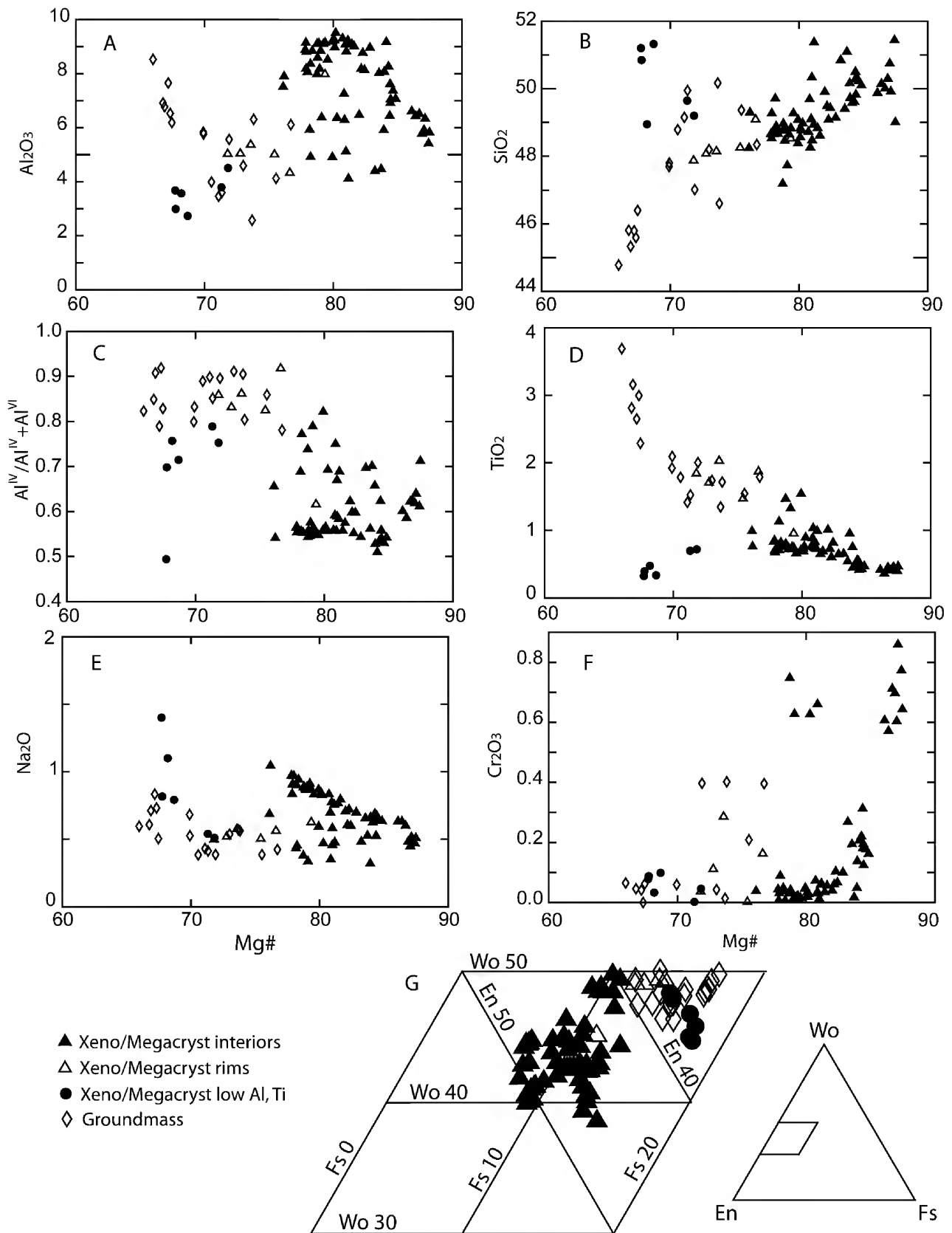


**Figure 4.** A-F Clinopyroxene chemical variation with Mg#. G. Plot of pyroxene quadrilateral compositions (uncorrected).



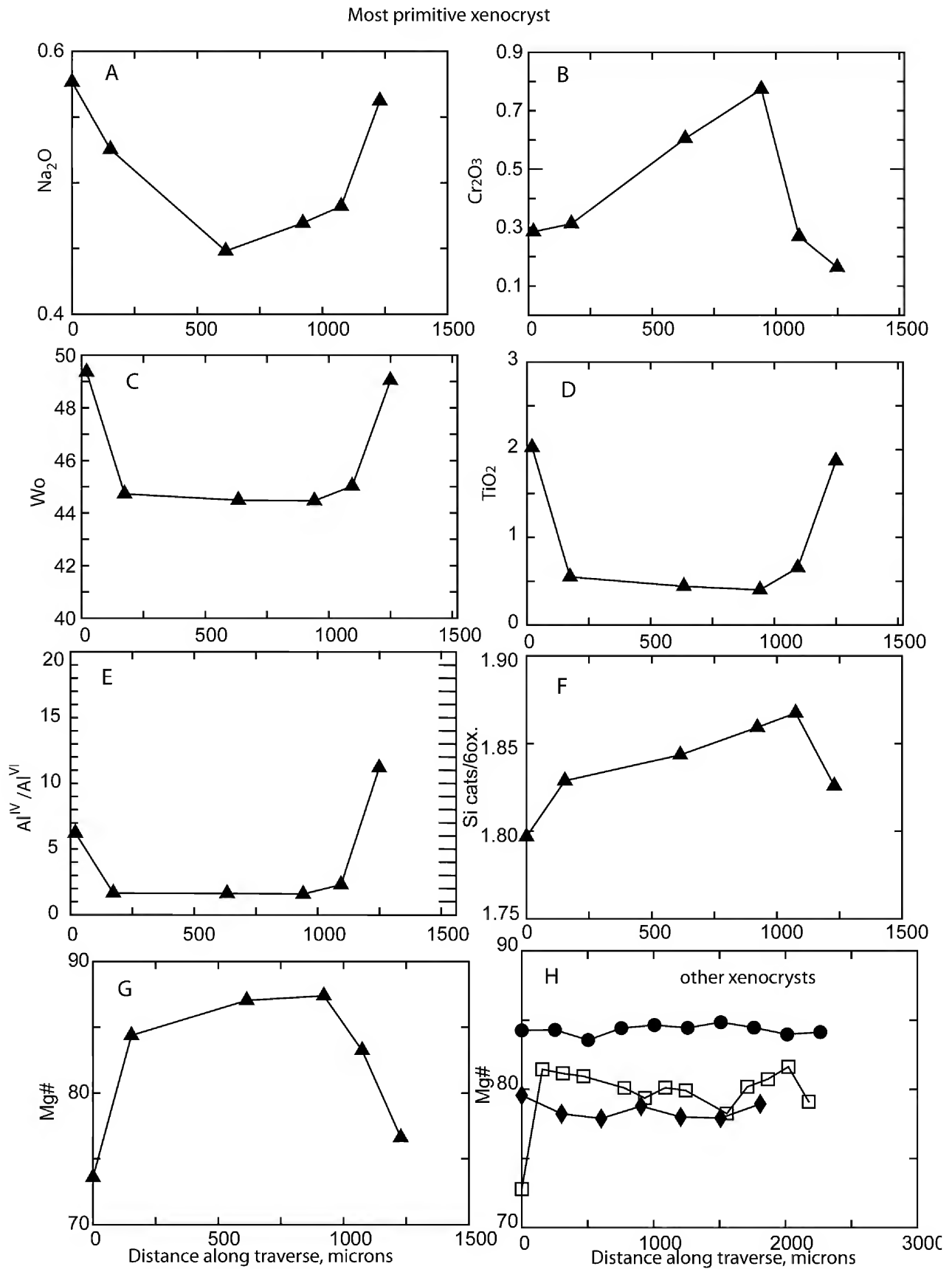


Figure 5. Chemical zoning along microprobe traverses. A-G, most Mg- and Cr-rich Clinopyroxene. H. Other clinopyroxene xenocrysts.

mm) rounded, pale greenish gray to nearly opaque crystals, with opacity correlating with total Fe. Most aluminous spinels are rounded, suggesting disequilibrium. The most Fe-rich aluminous spinels (e.g. Table 3, column 1) tend to be less rounded or even subhedral, but are also embayed. Aside from the rounding or embayment, the aluminous spinels show no other indication of reaction or overgrowth with the groundmass basalt. Aluminous spinels occur as single separate single crystals, or, less commonly, as inclusions in clinopyroxene. The spinels are very

poor in Cr ( $Cr\# < 1$ ) and have  $Fe^{+2}/(Fe^{+2}+Mg)$  ranging from 0.26 to 0.51. Ti and ferric iron increase with total iron. Mg# increases and ferric iron decreases with increasing Al (Figs. 6 and 7). Four individual xenocrysts were analyzed for this study and each has a distinct chemistry, with significant differences in Ti,  $Fe^{+2}$ ,  $Fe^{+3}$ , Mg, and Al content (Table 3). The spinel included in clinopyroxene is distinctly higher in Cr than the other aluminous spinels (Fig. 7). A single, very small, opaque, Cr-rich spinel ( $Cr/Cr+Al = 0.42$ ) was found as an inclusion in olivine (Fig. 6;

**Table 3: Spinel**

| VMNH#                          | 81564     | 81554     | 81554      | 81554     | 81554     | 81564      | 81564   | 81554   | 81554   | 81554   |
|--------------------------------|-----------|-----------|------------|-----------|-----------|------------|---------|---------|---------|---------|
| sample                         | Mh11      | Mh1-5-2   | Mh1-5-2    | Mh1-5-1   | Mh1-5-1   | Mh11       | Mh11    | Mh1-5-2 | Mh1-5-2 | Mh1-5-1 |
| n                              | 13        | 33        | 1          | 23        | 7         | 3          | 6       | 1       | 5       | 4       |
| x'l type                       | xenocryst | xenocryst | inclusion  | xenocryst | inclusion | phenocryst | grdmass | pheno?  | grdmass | grdmass |
| notes                          |           |           | in olivine |           | in cpx    | poikilitic |         |         |         |         |
| SiO <sub>2</sub>               | 0.11      | 0.13      | 0.13       | 0.10      | 0.14      | 0.10       | 0.16    | 0.09    | 0.09    | 0.20    |
| Al <sub>2</sub> O <sub>3</sub> | 54.58     | 65.08     | 30.73      | 58.81     | 63.07     | 6.31       | 4.28    | 6.30    | 2.08    | 2.21    |
| MgO                            | 13.27     | 20.04     | 14.62      | 15.55     | 19.50     | 4.62       | 3.40    | 4.30    | 1.76    | 2.11    |
| TiO <sub>2</sub>               | 0.96      | 0.27      | 0.62       | 0.55      | 0.31      | 14.65      | 18.75   | 13.95   | 18.09   | 17.78   |
| MnO                            | 0.20      | 0.10      | 0.13       | 0.17      | 0.10      | 0.53       | 0.66    | 0.51    | 0.85    | 0.83    |
| Cr <sub>2</sub> O <sub>3</sub> | 0.14      | 0.13      | 33.51      | 0.12      | 0.62      | 5.43       | 0.45    | 8.05    | 0.13    | 0.12    |
| Fe <sub>2</sub> O <sub>3</sub> | 12.18     | 4.38      | 5.48       | 8.06      | 5.09      | 29.83      | 28.59   | 28.71   | 31.39   | 30.80   |
| FeO                            | 22.15     | 12.87     | 15.19      | 18.47     | 13.06     | 38.25      | 43.47   | 38.30   | 44.40   | 43.33   |
| sum                            | 103.58    | 102.99    | 100.41     | 101.82    | 101.89    | 99.72      | 99.77   | 100.21  | 98.79   | 97.39   |
| <b>3 Cations/4 oxygens</b>     |           |           |            |           |           |            |         |         |         |         |
| Si                             | 0.003     | 0.003     | 0.004      | 0.003     | 0.004     | 0.003      | 0.006   | 0.003   | 0.003   | 0.008   |
| Al                             | 1.709     | 1.900     | 1.065      | 1.812     | 1.872     | 0.264      | 0.182   | 0.262   | 0.092   | 0.098   |
| Mg                             | 0.526     | 0.740     | 0.641      | 0.606     | 0.732     | 0.244      | 0.183   | 0.227   | 0.098   | 0.119   |
| Ti                             | 0.019     | 0.005     | 0.014      | 0.011     | 0.006     | 0.391      | 0.509   | 0.371   | 0.508   | 0.504   |
| Fe+3                           | 0.243     | 0.082     | 0.121      | 0.159     | 0.097     | 0.796      | 0.776   | 0.764   | 0.882   | 0.874   |
| Fe+2                           | 0.492     | 0.267     | 0.374      | 0.404     | 0.276     | 1.134      | 1.311   | 1.132   | 1.387   | 1.367   |
| Mn                             | 0.004     | 0.002     | 0.003      | 0.004     | 0.002     | 0.016      | 0.020   | 0.015   | 0.027   | 0.026   |
| Cr                             | 0.003     | 0.003     | 0.779      | 0.002     | 0.012     | 0.152      | 0.013   | 0.225   | 0.004   | 0.004   |
| total                          | 3.000     | 3.000     | 3.000      | 3.000     | 3.000     | 3.000      | 3.000   | 3.000   | 3.000   | 3.000   |
| Cr/Cr+Al                       | 0.002     | 0.001     | 0.422      | 0.001     | 0.007     | 0.351      | 0.064   | 0.462   | 0.039   | 0.036   |
| Mg#                            | 51.6      | 73.5      | 63.2       | 60.0      | 72.6      | 17.7       | 12.2    | 16.7    | 6.6     | 8.0     |
| <b>end-members</b>             |           |           |            |           |           |            |         |         |         |         |
| Mt                             | 0.122     | 0.041     |            | 0.079     | 0.048     | 0.276      | 0.288   | 0.278   | 0.369   | 0.356   |
| Uv                             | 0.019     | 0.005     | 0.014      | 0.011     | 0.006     | 0.391      | 0.509   | 0.371   | 0.508   | 0.504   |
| Cr                             | 0.001     | 0.001     | 0.389      | 0.001     | 0.006     | 0.076      | 0.006   | 0.113   | 0.002   | 0.002   |
| Sp                             | 0.520     | 0.733     | 0.529      | 0.601     | 0.725     | 0.116      | 0.071   | 0.116   | 0.019   | 0.023   |
| Gx                             | 0.004     | 0.002     | 0.003      | 0.004     | 0.002     | 0.016      | 0.020   | 0.015   | 0.027   | 0.026   |
| Hc                             | 0.331     | 0.215     | 0.000      | 0.301     | 0.209     | 0.000      | 0.000   | 0.000   | 0.000   | 0.000   |
| Mf                             | 0.000     | 0.000     | 0.104      | 0.000     | 0.000     | 0.122      | 0.100   | 0.104   | 0.072   | 0.081   |

Table 3). This Cr-spinel and all of the aluminous spinels plot in the fields of mantle xenoliths from alkali basalts as defined by Barnes and Roeder (2001) (Fig. 6).

Fe-Ti rich opaque spinels occur in the groundmass and as microphenocrysts in the Mole Hill microbasalt. Groundmass spinels can be classified as titanomagnetite (i.e. uv around 50 and

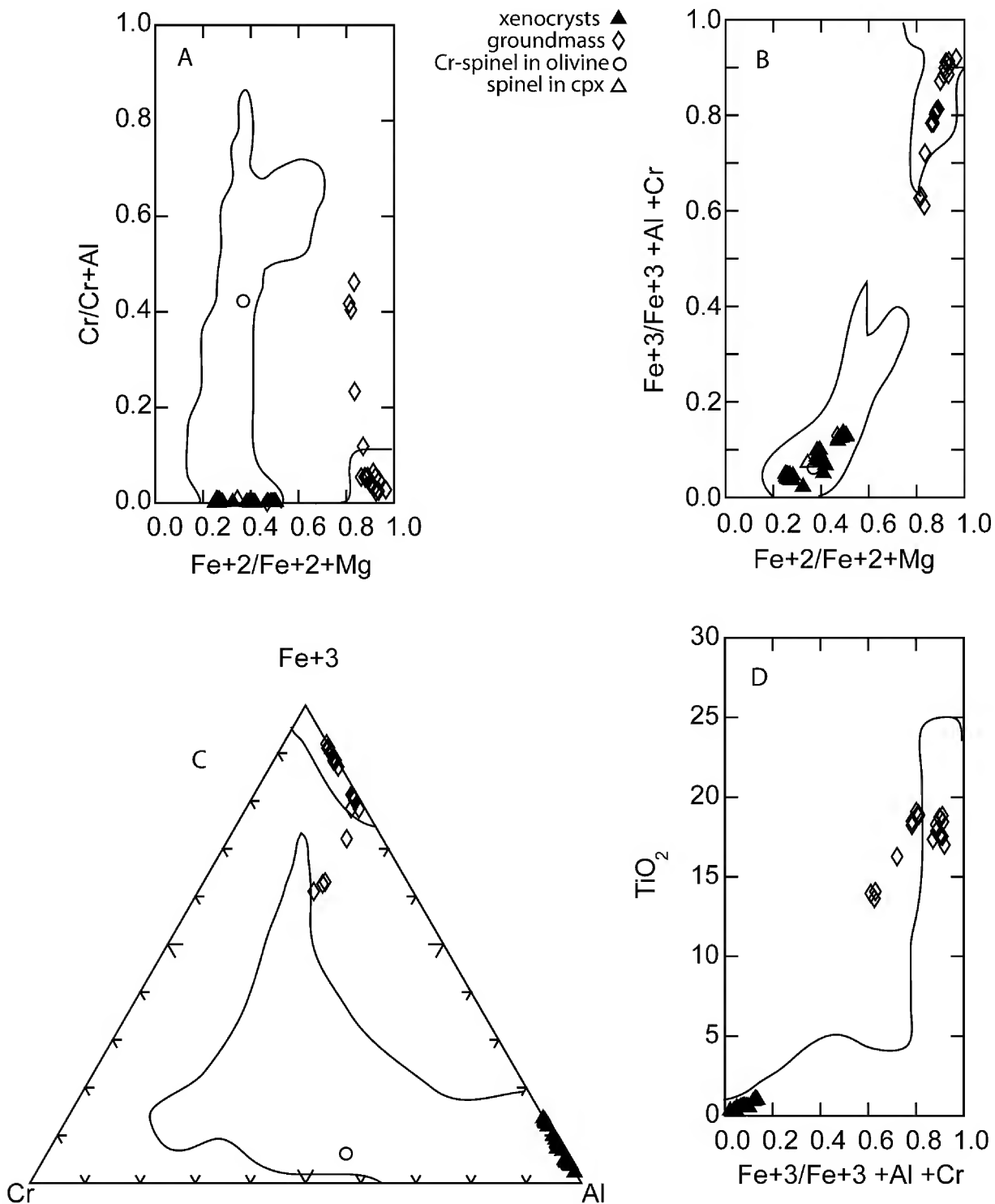
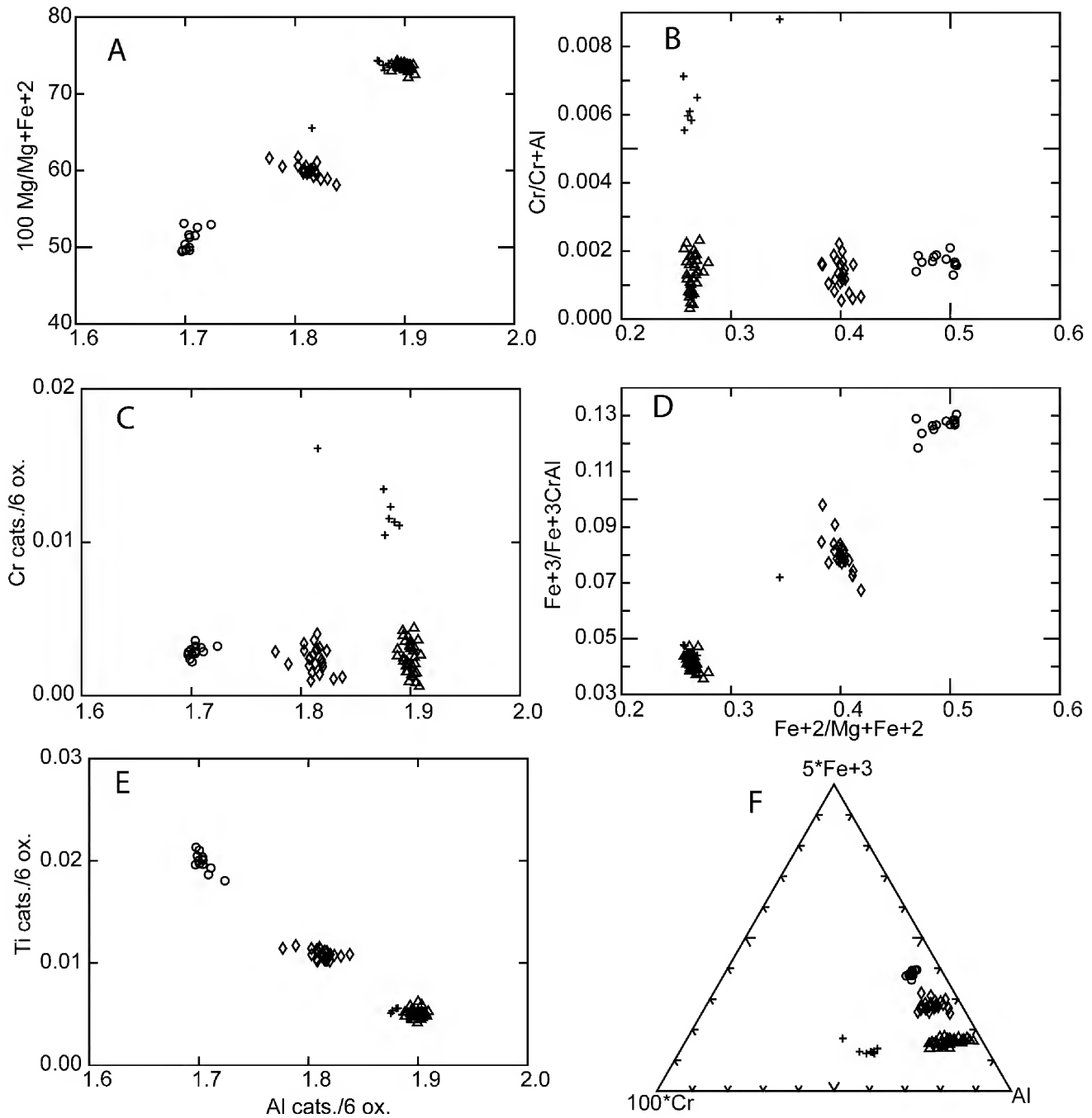


Figure 6. Spinel compositions in the Mole Hill microbasalt. Outlined fields are the fields of xenoliths in alkali basalts taken from Barnes and Roeder (2001).

mt+uv 78-92). Most have calculated magnesioferrite between 5 and 10% (Table 3). Poikilitic, opaque spinel microphenocrysts have chromite- (4-11%) and Mg-spinel- (10-12%) rich cores grading out to

titanomagnetite rims. The opaque spinels define trends of decreasing Mg and Cr and increasing followed by decreasing Ti as the magnetite component increases (Fig. 6). These spinels, at



**Figure 7.** Aluminous Spinel xenocrysts from the Mole Hill microbasalt. Individual groups of spots represent spot analyses from single crystals. Note the elevated Cr in the spinel included in clinopyroxene.

least in part, lie outside the basalt xenolith fields as defined by Barnes and Roeder (2001).

**Plagioclase.** Plagioclase occurs as micro-

phenocrysts, as inclusions in the rims of sieve-textured clinopyroxene rims, and as a groundmass phase in the Mole Hill microbasalts. Plagioclase is

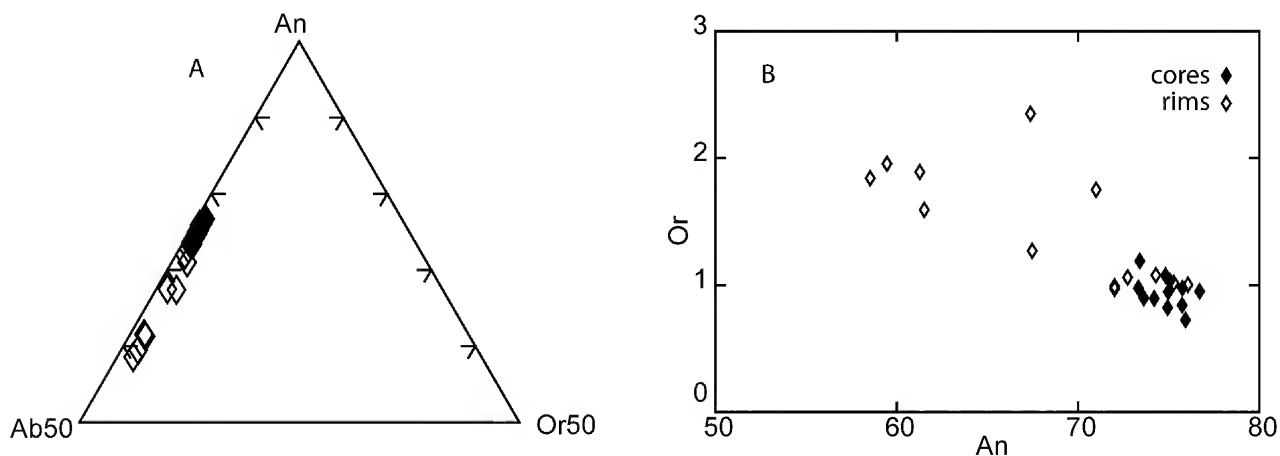


Figure 8. Plagioclase microphenocryst compositions, Mole Hill microbasalt.

Table 4: Plagioclase microphenocrysts

| VMNH#                    | 81564 | 81564  | 81554    | 81554    | 81554    | 81554    |        |
|--------------------------|-------|--------|----------|----------|----------|----------|--------|
| sample                   | Mh 11 | Mh 11  | Mh 1-5-2 | Mh 1-5-2 | Mh 1-5-1 | Mh 1-5-1 |        |
| n                        |       | 11     | 1        | 8        | 3        | 10       | 2      |
| notes                    | core  | rim    | core     | rim      | core     | rim      |        |
| SiO2                     |       | 48.25  | 52.67    | 48.79    | 51.22    | 48.43    | 51.30  |
| Al2O3                    |       | 32.17  | 29.71    | 32.23    | 30.76    | 31.85    | 30.15  |
| Na2O                     |       | 2.84   | 4.71     | 2.88     | 3.83     | 2.88     | 4.07   |
| K2O                      |       | 0.18   | 0.33     | 0.17     | 0.25     | 0.18     | 0.29   |
| CaO                      |       | 16.02  | 12.61    | 15.78    | 13.99    | 15.50    | 13.38  |
| FeO                      |       | 0.77   | 0.79     | 0.80     | 1.03     | 0.84     | 0.82   |
| sum                      |       | 100.23 | 100.82   | 100.65   | 101.09   | 99.68    | 100.01 |
| <b>Cations/8 oxygens</b> |       |        |          |          |          |          |        |
| Si                       |       | 2.218  | 2.383    | 2.230    | 2.321    | 2.235    | 2.344  |
| Al                       |       | 1.743  | 1.584    | 1.736    | 1.643    | 1.732    | 1.624  |
| Na                       |       | 0.253  | 0.414    | 0.255    | 0.336    | 0.257    | 0.361  |
| K                        |       | 0.011  | 0.019    | 0.010    | 0.015    | 0.010    | 0.017  |
| Ca                       |       | 0.789  | 0.611    | 0.773    | 0.680    | 0.766    | 0.655  |
| Fe                       |       | 0.030  | 0.030    | 0.031    | 0.039    | 0.033    | 0.031  |
| total                    |       | 5.043  | 5.041    | 5.034    | 5.033    | 5.033    | 5.032  |
| An                       |       | 75.0   | 58.5     | 74.5     | 65.9     | 74.1     | 63.5   |
| Ab                       |       | 24.0   | 39.6     | 24.6     | 32.7     | 24.9     | 34.9   |
| Or                       |       | 1.0    | 1.8      | 0.9      | 1.4      | 1.0      | 1.6    |

## DISCUSSION

zoned, with cores of An<sub>75</sub> and narrow rims ranging down to An<sub>38</sub> (Table 4, Fig. 8). Plagioclase is not observed to be in a reaction relationship with any megacryst phase.

#### **Origin of the megacrysts and xenocrysts.**

Taken as a group, the clinopyroxene and olivine megacrysts or xenocrysts from Mole Hill have compositions less evolved than typical mantle peridotites, even relatively fertile subcontinental lherzolites (e.g. Rudnick et al., 2004; Ackerman et al., 2007; Bjerg et al., 2009). On the other hand, many continental xenolith suites include a variety of clinopyroxene-rich ultramafic rocks such as clinopyroxenite, olivine clinopyroxenite, and wehrlite (Wilshire and Shervais, 1975; Irving, 1980; Ghent et al., 1980; Brearly et al., 1984; Kovacs et al., 2004; Rehfeldt et al., 2007; Xiao et al., 2010). Two groups of cpx-rich xenoliths are recognized, a Cr-diopside suite, which is typically dominated by rocks relatively rich in olivine (e.g. cpx-rich lherzolite) and an Al-augite suite in which cpx is generally the dominant mineral (Wilshire and Shervais, 1975; Irving, 1980). The Al-augite suite rocks occur as individual xenoliths, and, perhaps even more commonly, as veins intrusive into typical mantle peridotites in composite xenoliths. These cpx-rich veins reflect metasomatism of the lithosphere either by melts or fluids (Wilshire and Shervais, 1975; Irving, 1980)).

The megacrystic/xenocrystic olivine, cpx, and spinel at Mole Hill suggest an affinity with the Al-augite xenolith suite. First, the Mg# of both olivine and cpx are lower than would be expected for unmodified mantle and within the range observed in the Al-augite suite. Second, the low Cr<sub>2</sub>O<sub>3</sub> (most <0.4 wt.%) and high Al<sub>2</sub>O<sub>3</sub> (most >7 wt.%) in Mole Hill cpx are typical (and definitive) of the Al-augite suite (Wilshire and Shervais, 1975). Third, the Mole Hill

aluminous megacrystic spinels have exceptionally low Cr content and Cr#, among the lowest ever reported for putative mantle-derived spinels. Low Cr# (e.g. <10) spinels occur in a variety of xenolith suites (Fig. 5) (Barnes and Roeder, 2001), including Al-augite xenoliths. However, spinels with Cr#<3 appear to occur exclusively within the Al-augite suite (Wilshire and Shervais, 1975; Ghent et al., 1980; Brearly et al., 1984; Kovacs et al., 2004; Rehfeldt et al., 2007). The one feature of the Mole Hill megacryst suite that is atypical of the Al-augite suite is the relatively high NiO concentration in some Mole Hill olivine. One possible explanation for this is that the Ni-rich olivines represent fragments of the host peridotite, rather than the cpx-rich vein assemblage. The presence of a single Cr-rich spinel inclusion in one magnesian olivine megacryst is supportive of an origin distinct from the cpx and aluminous spinel megacrysts for at least some olivine.

#### **Implications of cognate mineral compositions for origin and evolution of the microbasalt.**

At present, no reliable whole-rock chemical data exists for the Mole Hill diatrema. The single analysis in Southworth et al. (1993) is of highly altered and contaminated rock. Some hints as to the nature of the magma, however, may be found in the compositions of microphenocryst and groundmass (cognate) minerals. The moderate Cr-content of some cognate cpx and titanomagnetite, the relatively calcic nature of the plagioclase, and the moderate (e.g. ~70) Mg# of cognate cpx and olivine all suggest derivation from a somewhat, but not extensively, evolved alkali basalt-type magma. A more detailed understanding of the petrogenesis of the magma awaits further mineral and, especially, whole-rock chemistry.

#### ACKNOWLEDGEMENTS

Thanks to Richard Hoffman and Elizabeth Johnson for a timely and constructive reviews. The

VMNH Foundation provided partial support for this project.

## REFERENCES CITED

- Ackerman, L., Mahlen, N., Jelínek, E., Medaris, G., Tlrych, J., Strnad, L., and Martin, M. (2007) Geochemistry and Evolution of Subcontinental Lithospheric Mantle in Central Europe: Evidence from Peridotite Xenoliths of the Kozákov Volcano, Czech Republic. *Journal of Petrology*, v.48, p.2235-2260
- Barnes, S.J., and Roeder, P.L. (2001) The Range of spinel compositions in terrestrial mafic and ultramafic rocks. *Journal of Petrology*, v. 42, p.2279-2302.
- Bjerg, E.A., Ntaflou, T., Thöni, M., Aliani, P., and Labudia, C.H. (2009) Heterogeneous Lithospheric Mantle beneath Northern Patagonia: Evidence from Prahuanique Garnet- and Spinel-Peridotites. *Journal of Petrology*, v.50, p.1267-1298.
- Brearley, M., Scarfe, C.M., and Fujii, T. (1984) The petrology of ultramafic xenoliths from Summit Lake, near Prince George, British Columbia. *Contributions to Mineralogy and Petrology* v.88, p.53-63.
- Costa, F. and Dungan, M. (2005) Short time scales of magmatic assimilation from diffusion modeling of multiple elements in olivine. *Geology*, v.33., p.837-840.
- Gerke, T.L., Kilinc, A.I. and Sack, R.O. (2005) Ti-content of high-Ca pyroxenes as a petrogenetic indicator: an experimental study of Mafic Alkaline Rocks from the Mt. Erebus volcanic region, Antarctica. *Contributions to Mineralogy and Petrology*, v.148 p.735-745.
- Ghent, E.D., Coleman, R.G., and Hadley, D.G. (1980) Ultramafic inclusions and host alkali olivine basalts of the southern coastal plain of the Red Sea, Saudi Arabia. *American Journal of Science*, v.280a, p.499-527.
- Harris, W.B., and Fullagar, P.D. (1989) Comparison of Rb-Sr and K-Ar dates of middle Eocene bentonite and glauconite, southeastern Atlantic Coastal Plain. *Geological Society of America Bulletin*, v. 101, p. 573-577.
- Hirano, N., Yamamoto, J., Kagi, H., and Ishii, T., (2004) Young, olivine xenocryst-bearing alkali-basalt from the oceanward slope of the Japan Trench. *Contributions to Mineralogy and Petrology*, v.148, p.47-54.
- Irving, A.J. (1980) Petrology and geochemistry of composite ultramafic xenoliths in alkalic basalts and implication for magmatic processes in the mantle. *American Journal of Science*, v.280a, p.389-426.
- Kovcás, I., Zajacz, Z., and Szabo, C. (2004) Type-II xenoliths and related metasomatism from the Nógrád-Gömör Volcanic Field, Carpathian-Pannonian region (northern Hungary-southern Slovakia), *Tectonophysics*, v.393, p.139- 161
- Rader, E. K., Gathright, T. M., II, and Marr, J. D., Jr. (1986) Trimble Knob basalt diatreme and associated dikes, Highland County, Virginia. Geological Society of America Centennial Field Guide – Southeastern Section, p. 97-100.
- Rehfeldt, T., Obst, K., and Johansson, L. (2007) Petrogenesis of ultramafic and mafic xenoliths from Mesozoic basanites in southern Sweden: constraints from mineral chemistry. *International Journal of Earth Science*, v.96, p.433-450
- Robinson, P. (1980) The compositional space of terrestrial pyroxenes – internal and external limits. In C.T. Prewitt (ed.) *Pyroxenes. Reviews in Mineralogy* v.7, Mineralogical Society of America, Washington D.C.
- Rohrbach, A., Schuth, S., Balhaus, C., Münker, C., Matveev, S., and Qopoto, C. (2005) Petrological constraints on the origin of arc picrites, New Georgia Group, Solomon Islands *Contributions to Mineralogy and Petrology*, v.149, p.685-698.
- Rudnick, R.L., Gao, S., Ling, W-L, Lui, Y-S, and McDonough, W.F. (2004) Petrology and geochemistry of spinel peridotite xenoliths from Hannuoba and Qixia, North China craton. *Lithos*, v.77, p.609- 637.
- Simkin, T. and Smith, J.V. (1970) Minor-element distribution in olivine. *Journal of Geology*, v.78, p. 304-325.
- Southworth, C. S., Gray, K. J., and Sutter, S. (1993) Middle Eocene intrusive igneous rocks of the

- central Appalachian Valley and Ridge province – setting, chemistry, and implications for crustal structure: *United States Geological Survey Bulletin*, Report B1839-I, J, p. J1-J24.
- Tso, J.L., and Surber, J.D. (2006) Eocene igneous rocks near Monterey Virginia: a field study. *Virginia Minerals*, v.49, no.3&4, p.9-24.
- Tso, J. L., McDowell, R. R., Avary, K. L., Matchen, D. L., and Wilkes, G. P. (2004) Middle Eocene igneous rocks in the Valley and Ridge of Virginia and West Virginia, in Southworth, S. and Burton, W., eds., *Geology of the National Capital Region: Field Trip Guidebook*, U. S. Geological Survey, Circular 1264, p. 137-161.
- Wilshire and Shervais (1975) Al-augite and Cr-diopside ultramafic xenoliths in basaltic rocks from western United States. *Physics and Chemistry of the Earth*, v.9, p.257-272.
- Wood D.A. (1980) The application of the Th-Hf-Ta diagram to problems of tectonomagmatic classification and to establish the nature of crustal contamination of the basaltic lavas of the British Tertiary Province. *Earth and Planetary Science Letters*, v.50, p.11-30.
- Xiao, Y., Zhang, H-F., Fan, W-M, Ying, J-F, Zhang, J, Zhao, X-M, and Su, B-X. (2010) Evolution of lithospheric mantle beneath the Tan-Lu fault zone, eastern North China Craton: Evidence from petrology and geochemistry of peridotite xenoliths. *Lithos*, v.117 p. 229–246.



*Parts published to date*

1. On the taxonomy of the milliped genera *Pseudojulus* Bollman, 1887, and *Georgiulus*, gen. nov., of southeastern United States. Richard L. Hoffman. Pp. 1-19, figs. 1-22. 1992. \$2.00
2. A striking new genus and species of bryocorine plant bug (Heteroptera: Miridae) from eastern North America. Thomas J. Henry. Pp. 1-9, figs. 1-9. 1993. \$1.00.
3. The American species of *Escaryus*, a genus of Holarctic centipeds (Geophilo-morpha: Schendylidae). Luis A. Pereira & Richard L. Hoffman. Pp. 1-72, figs. 1-154, maps 1-3. 1993. \$7.00
4. A new species of *Puto* and a preliminary analysis of the phylogenetic position of the *Puto* Group within the Coccoidea (Homoptera: Pseudococcidae). Douglass R. Miller & Gary L. Miller. Pp. 1-35, figs. 1-7. 1993. \$4.00.
5. *Cambarus* (*Cambarus*) *angularis*, a new crayfish (Decapoda: Cambaridae) from the Tennessee River Basin of northeastern Tennessee and Virginia. Horton H. Hobbs, Jr., & Raymond W. Bouchard. Pp. 1-13, figs. 1a-1n. 1994. \$2.00.
6. Three unusual new epigaeic species of *Kleptochthonius* (Pseudoscorpionida: Chthoniidae). William B. Muchmore. Pp. 1-13, figs. 1-9. 1994. \$1.50.
7. A new dinosauriform ichnogenus from the Triassic of Virginia. Nicholas C. Fraser & Paul E. Olsen. Pp. 1-17, figs. 1-3. 1996. \$2.00.
8. "Double-headed" ribs in a Miocene whale. Alton C. Dooley, Jr. Pp. 1-8, figs. 1-5. 2000. \$1.00.
9. An outline of the pre-Clovis Archeology of SV-2, Saltville, Virginia, with special attention to a bone tool dated 14,510 yr BP. Jerry N. McDonald. Pp. 1-60, figs. 1-19. 2000. \$3.00.
10. First confirmed New World record of *Apocyclops dengizicus* (Lepishkin), with a key to the species of *Apocyclops* in North America and the Caribbean region (Crustacea: Copepoda: Cyclopidae). Janet W. Reid, Robert Hamilton, & Richard M. Duffield. Pp. 1-23, figs. 1-3. 2002. \$2.50
11. A review of the eastern North American *Squalodontidae* (Mammalia: Cetacea). Alton C. Dooley, Jr. Pp. 1-26, figs. 1-6. 2003. \$2.50.
12. New records and new species of the genus *Diacyclops* (Crustacea: Copepoda) from subterranean habitats in southern Indiana, U.S.A. Janet W. Reid. Pp. 1-65, figs. 1-22. 2004. \$6.50.
13. *Acroneuria yuchi* (Plecoptera: Perlidae), a new stonefly from Virginia, U.S.A. Bill P. Stark & B. C. Kondratieff. Pp. 1-6, figs. 1-6. 2004. \$0.60.
14. A new species of woodland salamander of the *Plethodon cinereus* Group from the Blue Ridge Mountains of Virginia. Richard Highton. Pp. 1-22. 2005. \$2.50.
15. Additional drepanosaur elements from the Triassic infills of Cromhall Quarry, England. Nicholas C. Fraser & S. Renesto. Pp. 1-16, figs. 1-9. 2005. \$1.50.
16. A Miocene cetacean vertebra showing partially healed compression fracture, the result of convulsions or failed predation by the giant white shark, *Carcharodon megalodon*. Stephen J. Godfrey & Jeremy Altmann. Pp. 1-12. 2005. \$1.50.
17. A new *Crataegus*-feeding plant bug of the genus *Neolygus* from the eastern United States (Hemiptera: Heteroptera: Miridae). Thomas J. Henry. Pp. 1-10.
18. Barstovian (middle Miocene) Land Mammals from the Carmel Church Quarry, Caroline Co., Virginia. Alton C. Dooley, Jr. Pp. 1-17.
19. Unusual Cambrian Thrombolites from the Boxley Blue Ridge Quarry, Bedford County, Virginia. Alton C. Dooley, Jr. Pp 1-12, figs. 1-8, 2009.
20. Injuries in a Mysticete Skeleton from the Miocene of Virginia, With a Discussion of Buoyancy and the Primitive Feeding Mode in the Chaemysticeti. Brian L. Beatty & Alton C. Dooley, Jr., Pp. 1-28, 2009.
21. Morphometric and Allozymic Variation in the Southeastern Shrew (*Sorex longirostris*). Wm. David Webster, Nancy D. Moncrief, Becky E. Gurshaw, Janet L. Loxterman, Robert K. Rose, John F. Pagels, and Sandra Y. Erdle. Pp. 1-13, 2009.
22. Karyotype designation and habitat description of the northern short-tailed shrew (*Blarina brevicauda*, Say) from the type locality. Cody W. Thompson and Justin D. Hoffman, Pp. 1-5, 2009.
23. Diatom biostratigraphy and paleoecology of vertebrate-bearing Miocene localities in Virginia. Anna R. Trochim and Alton C. Dooley, Jr. Pp. 1-11, 2010.
24. A middle Miocene beaked whale tooth Caroline County, Virginia (Cetacea: Ziphiidae) from the Carmel Church Quarry, Virginia, and implications for the evolution of sexual dimorphism in ziphiids. Alton C. Dooley, Jr. Pp. 1-11. 2010.



*Virginia Museum of*  
**NATURAL HISTORY**

---

PUBLICATIONS

21 Starling Avenue  
Martinsville, VA 24112